ELSEVIER

Earth and Planetary Science Letters 183 (2000) 121–132

EPSL

www.elsevier.com/locate/epsl

The Poisson ratio of the Australian crust: geological and geophysical implications

Sébastien Chevrot, Robert D. van der Hilst *

Department of Earth, Atmospheric and Planetary Sciences, Massachusetts Institute of Technology, Rm. 54-514, Cambridge, MA 02139-4307, USA

Received 10 April 2000; received in revised form 19 July 2000; accepted 17 August 2000

Abstract

The Poisson ratio, which depends on the V_P/V_S ratio, provides much tighter constraints on the crustal composition than either the compressional or the shear velocity alone. The crustal Poisson ratio can be determined from the joint analysis of the travel times of waves converted at the Moho and of crustal multiples reflected at the top of the Moho. We have analyzed the records of the permanent stations installed on the Australian continent, complemented by the data of the SKIPPY experiment. The results reveal substantial variations in the Poisson ratio in the different tectonic units. For the Proterozoic crust, an increase of the Poisson ratio with increasing crustal thickness is systematically observed while for the Phanerozoic crust, the Poisson ratio tends to decrease for increasing crustal thicknesses. These observations are in remarkable agreement with the results of the deep seismic soundings that were performed in the former Soviet Union. The variations observed in the Proterozoic provinces can perhaps be explained by underplating of mafic materials at the base of the crust.

Keywords: Poisson's ratio; crust; Australia; S-waves; P-waves; composition

1. Introduction

As a consequence of their complex tectonic history, continents are characterized by large lateral variations in thickness and composition of the crust. The composition of the lower crust, an important factor in the determination of the average crustal composition and the understanding of crustal growth [1], is still poorly constrained [2]. This results from the great diversity of granulite terrains and xenoliths and the nonunique interpretation of seismic data in terms of rock type when compressional velocities alone are available [3]. Measuring crustal shear velocities is very important because the ratio between compressional and shear velocities discriminates between different rocks that have the same compressional velocities [4]. Therefore, the analysis of seismic wave velocities is a powerful tool to complement the petrological and geochemical studies in the investigation of the composition of the crust as well as its formation and evolution processes.

Different techniques have been used to study the crust. Refraction experiments provide accurate estimates of crustal thickness and compres-

* Corresponding author. Tel.: +1-617-253-6977; Fax: +1-617-253-7651; E-mail: hilst@mit.edu

0012-821X/00/$ – see front matter
PII: S0012-821X(00)00264-8

sional velocity. Reliable studies are expensive, however, and involve detailed data analysis and extensive modeling of both travel times and amplitudes of crustal body waves. Moreover, these studies rarely report shear wave velocities because seismic refraction experiments commonly use short period vertical seismometers from which it is difficult to pick the S arrivals. Additionally, they usually suffer from limited lateral resolution because the structure is averaged along the entire refraction line. Single-station techniques, based on the analysis of receiver functions, overcome most of these difficulties. First, they allow the utilization of high quality broadband seismograms that are recorded by the permanent stations of the global networks. Second, they offer very good lateral resolution. The principle of these techniques is to use the phases converted at the Moho and their multiples. Clarke and Silver [5] performed a waveform inversion of the P wave and its coda to determine the thickness and the Poisson ratio (σ) of the crust under six stations in North America. From the ratio between *Ps–P* and *PpPms–P* differential travel times (see Fig. 1 for the identification of these phases), Zandt and Ammon [6] determined σ using 76 stations distributed world wide. They found the highest σ (0.29) for shield crust and the lowest (0.25) for Cenozoic and Mesozoic crust, but the large number of outliers with σ larger than 0.30 casts some doubt about the validity of their measurements for many stations. It is possible that these outliers are due to the poor precision with which the onsets of *Pms* and *PpPms* phases can be picked on individual traces low pass filtered at 3 s.

In this study, we present new measurements for the Australian crust, exploiting the excellent coverage offered by the SKIPPY experiment [7], the permanent stations of the Global Seismographic Network (GSN), the Australian Geological Survey Organisation (AGSO), and the GEOSCOPE network. The crustal structure in the eastern part of Australia was previously investigated using a genetic algorithm inversion of receiver functions by Shibutani et al. [8]. Clitheroe et al. [9] later extended this analysis to the whole Australian continent. In these studies, stacked receiver functions are inverted to retrieve the shear wave velocity profile and the ratio between P and S wavespeeds (the V_P/V_S ratio) in the upper, middle and lower crust. We introduce a different technique and focus on measuring two parameters that describe the crust: the average crustal V_P/V_S ratio and the crustal thickness, defined by the Moho depth. The ability to determine accurately these two parameters depends critically on the crustal multiples generated at the Moho [10]. These phases have significant moveouts with respect to the P wave and will thus stack incoherently, leading to broader pulses and lower amplitudes in the receiver function stacks, which reduces the ability to extract information from them. In contrast, we perform receiver function stacks along the travel time curves of the converted and reflected phases at the Moho. We believe that this technique provides better constraints on the average V_P/V_S ratio, but because of the strict data selection criteria, not all stations can be analyzed. The comparison with crustal thicknesses obtained from nearby seismic refraction studies shows good agreement, which suggests that our σ measurements are reliable. Finally, we consider these observations with other constraints, such as the age of the crust, and discuss the geological and geophysical implications for our understanding of the structure and evolution of the continental crust.

2. The Poisson ratio and the composition of the crust

The Poisson ratio σ is related to the P and S wavespeeds ratio V_P/V_S via the relation:

$$\sigma = \frac{1}{2}(1-[(V_P/V_S)^2-1]^{-1}) \quad (1)$$

Laboratory experiments (see Christensen [4] for a review) have shown that many physical and chemical factors can induce variations of the average crustal Poisson ratio. For pressures larger than about 100–200 MPa the effects of cracks and porosity become negligible and σ does not show significant variations with pressure. In addition, σ also shows little variation with temperature. On the other hand, the mineralogy of rocks plays

an important role. The abundance of quartz ($\sigma = 0.09$) and plagioclase feldspar ($\sigma = 0.30$) have a dominant effect on the Poisson ratio of common igneous rocks. An increase of plagioclase content and a decrease of quartz content can usually explain the Poisson ratio increase, for example from about 0.24 for a granitic rock to 0.27 for a diorite, and 0.30 for a gabbro [11]. In general, an anticorrelation between the Poisson ratio and silica content is observed for rocks with SiO_2 contents above 55% [4]. Similarly, the variations of σ for metamorphic rocks are dominated by the abundance of quartz and anorthite. High metamorphic grades such as granulites are characterized by large values of σ (~ 0.29). The transition from granulite to quartz-enriched eclogite, which may explain the seismic velocity increase at the Moho, would manifest itself by a significant drop of σ. A Poisson ratio larger than 0.30 is rare in crustal rocks, except for serpentinite, for which σ can be as high as 0.35. Partial melt has also an important effect on the V_P/V_S ratio, which increases with an increasing fluid fraction [12]. The amplitude of the variations depend on the shape of the fluid inclusions. For a granite with 5% partial melt, located in randomly oriented triangular tubes, σ is around 0.31, compared to $\sigma = 0.24$ for a granite without melt. Therefore, crustal Poisson ratios greater than 0.30 are usually interpreted as evidence for extensive crustal melting [13].

3. Data analysis

As Zandt et al. [14] pointed out, it is possible to measure the crustal thickness and the Poisson ratio σ from the analysis of the travel times of the *Pms* (the *P* to *S* conversion at the Moho) and the *PpPms* (the first Moho multiple) phases, which both arrive in the coda of the *P* wave (Fig. 1). Receiver function analysis is an elegant way to isolate these phases and constrain the crustal wavespeeds and thickness. To generate receiver functions, the three *Z*, *N* and *E* components are first rotated to the *L* (longitudinal), *SV* and *SH* axis. *L* is along the *P* principal motion direction, *SV* is in the *P* propagation plane and is normal to

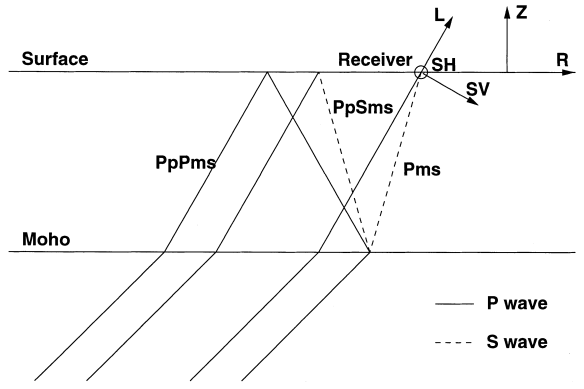

Fig. 1. Schematic ray diagram of the *Pms* phase, converted from *P* to *S* at the Moho. Also shown are the first multiple, *PpPms*, transmitted as *P*, reflected from the free surface as *P*, and reflected from the Moho as *S* and the second multiple, *PpSms*, transmitted as *P*, reflected from the free surface as *S* and reflected from the Moho as *S*. Axis *L* corresponds to the principal direction of the *P* wave particle motion. Axis *SV* is perpendicular to the axis *L* and is optimum for detecting the *Pms* phases. Axis *SH* is orthogonal to both *L* and *SV*.

L, and *SH* is normal to both *L* and *SV* (see Fig. 1). The longitudinal component is then deconvolved from the *L*, *SV* and *SH* components. The deconvolution procedure suppresses the effects of the source (location, source time function, radiation pattern) and aspherical mantle structure along the path before the converting interface. The resulting *SV* trace is called a receiver function and contains all the information related to the *P*–*SV* conversions and reflections at the seismic discontinuities beneath the station. Let us define t_1, the differential travel time between *Pms* and *P*, and t_2, the differential travel time between *PpPms* and *P*:

$$t_1 = \frac{H}{V_P}\left(\sqrt{\frac{V_P^2}{V_S^2} - p^2 V_P^2} - \sqrt{1 - p^2 V_P^2}\right) \quad (2)$$

$$t_2 = \frac{H}{V_P}\left(\sqrt{\frac{V_P^2}{V_S^2} - p^2 V_P^2} + \sqrt{1 - p^2 V_P^2}\right) \quad (3)$$

where V_P and V_S are the average *P* and *S* crustal velocities, respectively, *H* is the crustal thickness and *p* is the ray parameter. Thus, t_1 and t_2 depend on three crustal parameters: V_P, V_P/V_S, and *H*.

The form of Eqs. 2 and 3 shows that there is a trade-off between V_P and H. In theory, this trade-off could be resolved if many incident angles (or equivalently very different ray parameters) were available. Unfortunately, in practice, the analysis of earthquakes in the teleseismic distance range does not provide sufficient variations of the incident angles. However, it is possible to consider realistic mean crustal V_P to resolve the crustal thickness with a precision of the order of a few kilometers. Christensen and Mooney [3] calculated a mean crustal compressional velocity of 6.45 km/s from laboratory measurements of the velocities of different crustal rocks and their relative global abundance. Refraction experiments also provide reliable estimates of the average compressional crustal velocities. A review of the seismic refraction studies in Australia by Drummond and Collins [15] gives average crustal velocities between 6.4 and 6.5 km/s for the Archean cratons, and between 6.6 and 6.7 km/s for the Proterozoic and Phanerozoic provinces. The mean V_P does not appear to show significant variations with the age of the crust and is therefore not a critical parameter in our analysis. In the present study, we have chosen a value of 6.4 km/s for the Archean crust and a value of 6.6 km/s for the Proterozoic and Phanerozoic crust. Thus, we are left with a problem of determining H and V_P/V_S. For a better precision of the measurements, we determine these two parameters by stacking the amplitude of the receiver functions along the two travel time curves giving t_1 and t_2. H and V_P/V_S are allowed to vary between 20 and 60 km, and between 1.5 and 2.1, respectively. We look for the combination of parameters H and V_P/V_S that will give the maximum amplitude of the stack. Our approach is essentially the same as in Zhu and Kanamori [16], the only difference being that we assign equal weights to both travel time curves. As a consequence of a greater difficulty in observing *PpPms* than *Pms*, down-weighing the former compared to the latter, a choice made by Zhu and Kanamori [16] in order to weight each phases according to their signal-to-noise ratio (S/N), can result in a significant loss of sensitivity and precision in the measurements. Adopting strict data quality criteria, we can select records with reasonably good S/N even for the *PpPms* phase, which allows us to retain the full potential of the technique by assigning equal weights to both phases.

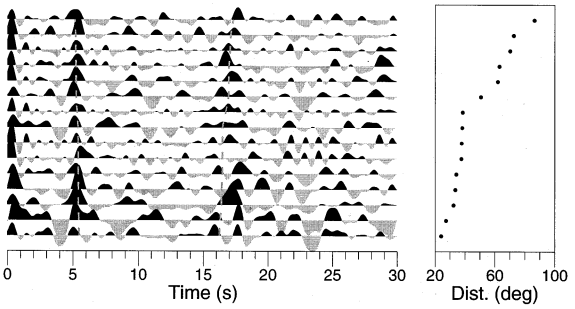

Fig. 2. *SV* component of receiver functions recorded by station SD02, sorted according to increasing epicentral distances. The gray dashed lines show the arrival times of the *Pms* and *PpPms* phases as predicted by the crustal parameters that give the maximum amplitude of the stacks in Fig. 3.

The stations can be classified into three categories. The first category corresponds to stations for which the *Pms* and *PpPms* phases are clearly visible on the receiver functions. The second category corresponds to stations where the phases can be detected and a clear maximum in the V_P/V_S versus H diagram obtained even though phase identification may be difficult. The third category corresponds to stations for which the records are too

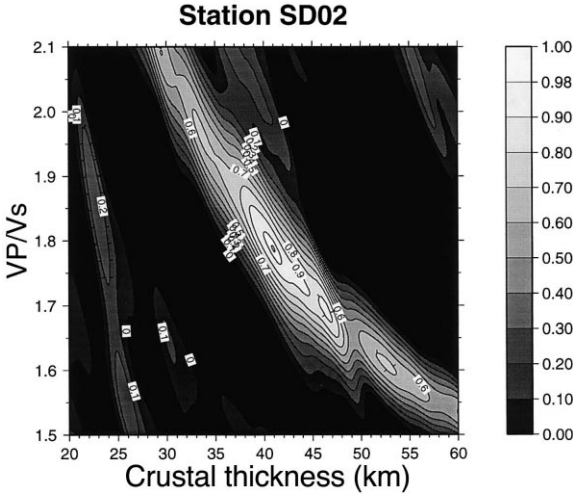

Fig. 3. Normalized amplitudes of the stacks along the two travel time curves corresponding to the *Pms* and *PpPms* phases.

complex or too noisy to measure V_P/V_S and H with sufficient confidence. In this study, only the stations in the first two categories are kept for further analysis. Fig. 2 shows a selection of receiver functions recorded by station SD02. The time $t=0$ corresponds to the P wave arrival. Both the conversion at the Moho, arriving around 5 s after the P wave, and the *PpPms*, arriving around 17 s after the P wave, are clearly visible. Therefore, this station is classified in the first category. The gray dashed lines correspond to the travel time curves of the *Pms* and *PpPms* phases. These curves are derived from Eqs. 2 and 3 using the crustal parameters H and V_P/V_S that give the maximum amplitude of the stacks, shown in Fig. 3. The fluctuations around these average curves reflect the lateral variations of the crust, which do not appear very severe under station SD02.

This operation was performed for all stations that could provide reliable measurements. After a careful examination of the data recorded by the permanent stations of the global (IRIS, GEOSCOPE) and regional (AGSO) networks, augmented by the stations installed during the SKIPPY project [7], 28 stations were selected for the present study (Fig. 4) out of an initial set of 70 stations. A coarse regionalization of the continent was made following Simons et al. [17], whereby Australia is divided in a Western part, predominantly Archean, a Central part, predominantly Proterozoic, and an Eastern part which includes the regions to the East of the Tasman line, which are Phanerozoic in age. The Tasman line marks the limits between the Proterozoic and Phanerozoic terranes. The Interior Lowlands form a major drainage system, characterized by a thick sedi-

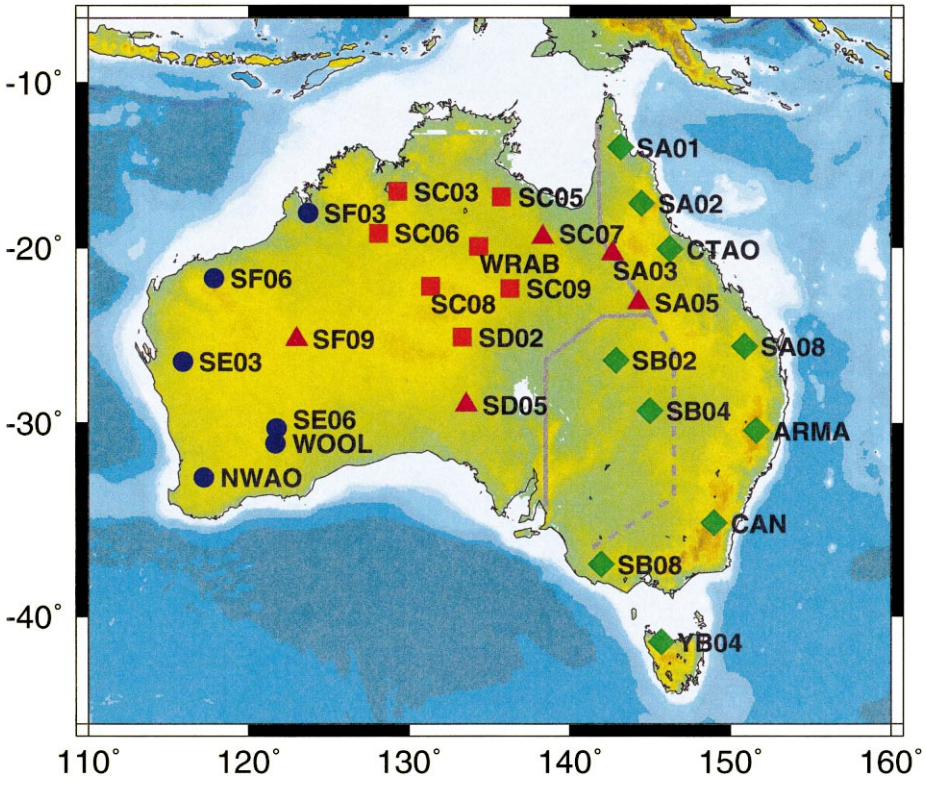

Fig. 4. Map of stations in the Archean (blue circles), Proterozoic (orange squares and magenta triangles) and Phanerozoic (green diamonds) for which we could make the measurements (categories 1 or 2). The solid gray line is the eastern edge of the high shear wavespeeds determined from Simons et al. [17] that we associate with the limit of the Proterozoic shield. The dashed gray line marks the western edge of the low lithospheric wavespeeds beneath the Australian sea board [17].

Table 1
Results of the receiver function analysis for each station

Station	Net. affil.	Latitude	Longitude	H (km)	V_P/V_S	σ	Nb. traces	Qual.
SA01	SKIPPY	−13.96	143.18	38	1.69	0.23	17	1
SA02	SKIPPY	−17.36	144.49	32	1.72	0.25	9	2
SA03	SKIPPY	−20.34	142.67	38	1.78	0.27	27	1
SA05	SKIPPY	−22.94	140.14	26	1.73	0.25	19	1
SA08	SKIPPY	−25.71	150.89	36	1.73	0.25	22	1
SB02	SKIPPY	−26.51	142.89	28	1.84	0.29	8	1
SB04	SKIPPY	−29.34	145.01	39	1.71	0.24	10	2
SB08	SKIPPY	−37.43	141.98	31	1.81	0.28	10	2
SC03	SKIPPY	−16.63	129.32	41	1.72	0.25	17	1
SC05	SKIPPY	−16.97	135.78	58	1.81	0.28	20	2
SC06	SKIPPY	−19.14	128.12	39	1.70	0.24	32	1
SC07	SKIPPY	−19.37	138.33	42	1.81	0.28	13	1
SC08	SKIPPY	−22.27	131.37	43	1.71	0.24	22	2
SC09	SKIPPY	−22.40	136.30	52	1.82	0.28	9	2
SD02	SKIPPY	−25.19	133.33	44	1.74	0.25	15	1
SD05	SKIPPY	−29.00	133.59	40	1.77	0.27	20	1
SE03	SKIPPY	−26.58	115.91	33	1.82	0.28	5	1
SE06	SKIPPY	−30.28	121.77	41	1.74	0.25	2	1
SF03	SKIPPY	−17.94	123.73	33	1.82	0.28	4	1
SF06	SKIPPY	−21.80	117.86	30	1.82	0.28	3	1
SF09	SKIPPY	−25.29	123.01	41	1.76	0.26	7	1
YB04	SKIPPY	−41.23	145.70	39	1.72	0.25	8	1
ARMA	AGSO	−30.42	151.63	34	1.74	0.25	21	1
WOOL	AGSO	−31.10	121.70	38	1.75	0.26	14	1
CAN	GEOSCOPE	−35.32	149.00	37	1.72	0.25	135	1
WRAB	IRIS	−19.93	134.36	48	1.73	0.25	33	1
CTAO	IRIS	−20.09	146.25	34	1.81	0.28	55	1
NWAO	IRIS	−32.93	117.23	39	1.82	0.28	24	1

mentary cover, up to 3.5 km thick [18]. As a result, the limited exposure of the basement in central east Australia makes the identification of the Tasman line difficult. Here, we also use the term 'Tasman line' in this conventional sense, but we define the eastern edge of the Proterozoic shield not on the basis of surface outcrop but on lateral variations in seismic wavespeeds in the lithosphere as inferred from surface wave tomography. For this, we use the upper mantle models produced by Simons et al. [17]. The eastern edge of the shield is not a vertical but a complicated 3D surface; the Tasman line depicted in Fig. 4 (solid gray line) is based on the wavespeed contrasts at 80 and 120 km depth. The dashed gray line in Fig. 4 marks the western edge of the low lithospheric wavespeeds beneath the Australian sea board. Table 1 summarizes the measurements for the 28 stations that were kept for the analysis. Fig. 5 shows the stations that could not be used because of the absence of crustal multiples (empty circles) or because of the absence of both the P to S conversion at the Moho and the crustal multiples (empty squares). Due to technical problems during the last stage of the SKIPPY experiment, very few data are available for the western Archean provinces.

4. The crustal thickness: comparison with seismic refraction studies

In order to assess the quality of our measurements, we have compared the crustal thicknesses obtained from receiver function analysis with the crustal thicknesses determined from nearby seismic refraction studies compiled by Collins [19]. For some stations close measurements are not

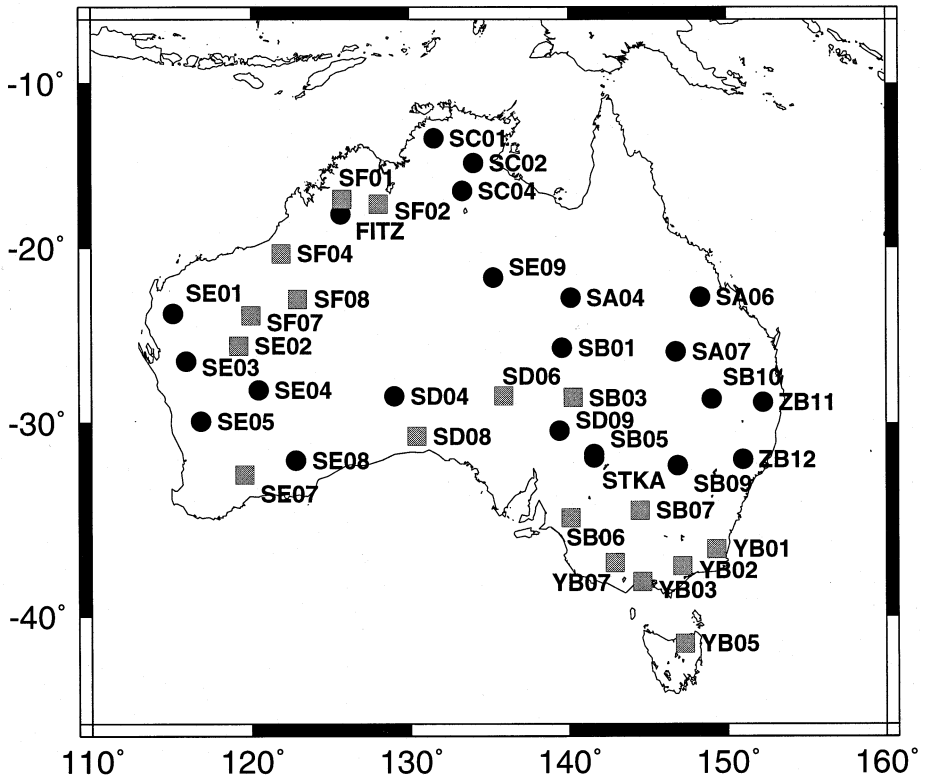

Fig. 5. Station map showing the stations that could not be used for the present study (category 3). The empty circles correspond to the stations for which the conversion at the Moho was visible but for which no clear multiple could be detected. The empty squares correspond to the stations for which no conversion at the Moho could be detected reliably.

available and these stations are therefore excluded from this comparison. Fig. 6 shows that by assuming realistic values for the mean crustal compressional velocities, receiver functions and seismic reflection studies agree well with each other, with a correlation coefficient of 0.83. The only significant outliers are station WRAB and station SC07 (see Fig. 4). Even when these two stations are included, the root mean square of the difference is only 4 km. The observed differences can be accounted for by a combination of different factors. First, the seismic refraction experiments and the receiver functions do not sample the crust at exactly the same locations, and the two techniques have very different lateral resolution since seismic refraction averages the structure along 200–300 km long traverses whereas receiver functions constrain the structure immediately below the station in a range of about 10–20 km. Second, we are

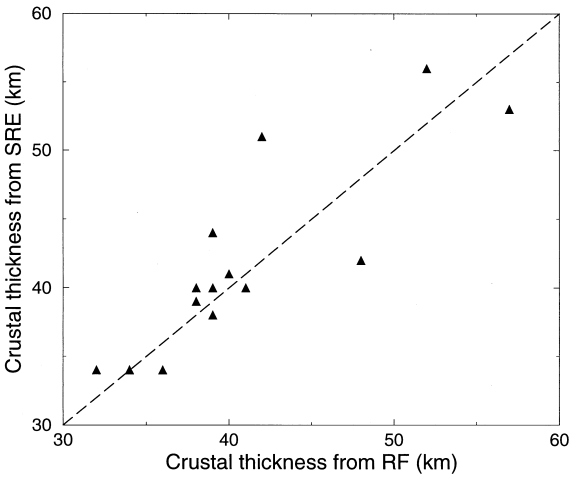

Fig. 6. Comparison between the crustal thicknesses obtained from our receiver function (RF) analysis and from seismic refraction experiment (SRE).

comparing average crustal properties that are constrained by P waves for the seismic refraction experiments, and by a combination of P and S waves for the receiver functions. If the V_P/V_S ratio varies with depth, then the two techniques will not average the crust in the same manner. Third, under stations like CAN, where broad *Pms* phases are observed in the receiver functions, the Moho forms a broad transition from the lower crust to the upper mantle. Clitheroe et al. [9] define the Moho as the boundary where $V_P > 7.6$ km/s. In such cases, significant differences are expected between their estimates of crustal thicknesses and ours. Additionally, the Moho depth estimated by waves refracted below the Moho (with typical mantle velocities $V_P > 8.0$ km/s) will tend to be larger than the crustal thickness estimated from receiver functions. In conclusion, since the different techniques rely on different definitions for the Moho and sample the crust differently, some care should be taken when comparing and combining the different kinds of measurements. Nevertheless, with all these restrictions in mind, this comparison demonstrates that receiver function analysis is well suited for a reliable and efficient survey of the average properties of the crust.

5. Error estimates

The determination of the measurement error is important to assess our ability to actually resolve the observed regional variations of the V_P/V_S ratio and crustal thickness. We estimate the errors by a bootstrap analysis [20]. Briefly, N receiver functions are randomly selected among a complete set of N receiver functions available for a given station. For each realization, the measured V_P/V_S ratio and crustal thickness correspond to the values that give the maximum amplitude of the stack. With our approach, the V_P/V_S ratio and the crustal thickness estimates are anticorrelated. This anticorrelation is clearly seen in Fig. 3. As a result, the ellipses which represent the one standard deviation confidence interval have their first principal axes following a negative slope (see Fig. 7). The main result of the error analysis is that the observed variations are indeed much larger than the measurements uncertainty from which we conclude that they must reflect some real and fundamental characteristics of the crust.

6. Results

In the next step, we compare the crustal thicknesses and V_P/V_S ratios measured at individual stations. Clitheroe et al. [9] and Shibutani et al. [8] have determined crustal V_S and V_P/V_S profiles from a genetic algorithm inversion of receiver functions stacks but they only show the V_P/V_S for four different stations (only two of which are present in our analysis). Therefore, it is impossible to make a detailed comparison between their results and ours. Additionally, if their approach gives reliable estimates of the Moho depth, it is probably not suited for constraining V_P/V_S. As described above, V_P/V_S can only be constrained if the *PpPms* is detected. Since *PpPms* can have significant moveouts with respect to the P wave, its amplitude in their stacks will be small, making the V_P/V_S estimates unreliable. Indeed, no clear evidence of crustal multiples can be observed in the stacked radial receiver functions shown by Clitheroe et al. [9] and Shibutani et al. [8].

Without further characterization of the stations, the analysis does not show a statistically significant correlation between V_P/V_S and H or between V_P/V_S and the age of the crust. However, surprizing relationships are revealed when the stations are separated into three different groups corresponding to the Archean (blue circles), Proterozoic (magenta triangles and orange squares) and Phanerozoic provinces (green diamonds) (Figs. 4 and 7). Clear contrasts are observed between the different provinces. The Archean crust is thinner than the Proterozoic crust, with an average thickness of about 35 km, in contrast to an average thickness of about 45 km for the latter. This observation is in very good agreement with the compilation of crustal thicknesses in Australia obtained by seismic refraction [15] and with a previous receiver functions study [9]. Durrheim and Mooney [21] compared crustal models from many parts of the world and concluded that in general, Proterozoic provinces have a thicker

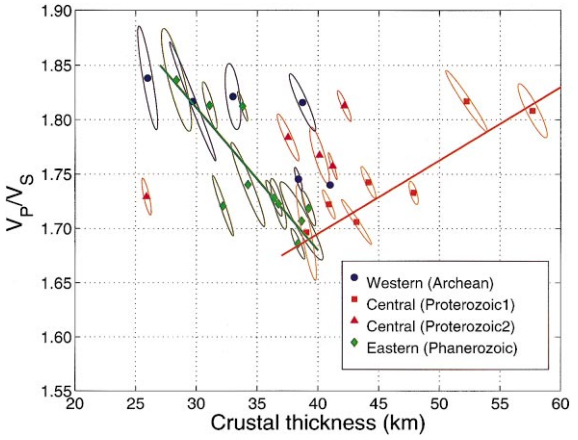

Fig. 7. Measured V_P/V_S ratios as a function of crustal thickness for the stations in the Archean (blue circles), Proterozoic (orange squares and magenta triangles) and Phanerozoic provinces (green diamonds). For station locations and measurements see Fig. 4 and Table 1.

crust than the Archean provinces and that they have a greater proportion of material with seismic velocities greater than 7 km/s. The V_P/V_S is also different between the Archean crust and the Proterozoic crust. For the Archean, we find a bimodal distribution of V_P/V_S. Stations SE06 and WOOL, which are very close to each other, have a low $V_P/V_S \sim 1.74$. For the other stations in the Archean, we measure consistently a high $V_P/V_S \sim 1.82$. The Yilgarn and Pilbara cratons result from a long and complex Precambrian history and are very heterogeneous [22]. Our limited sampling prevents any attempt to relate V_P/V_S with the nature of the Archean crust. However, we find the highest V_P/V_S in the Archean terranes which would suggest rather mafic compositions for the Archean crust. The V_P/V_S ratio also displays some variability in the Proterozoic crust but two groups of stations can be identified: Proterozoic 1 and Proterozoic 2 (marked by orange squares and magenta triangles, respectively, in Fig. 7). The first group is defined by the stations on the North Australian craton. The second group is defined by stations on the northeastern orogens and the Central Australian mobile belts regions (see Fig. 1 in Collins [19]). In these regions the Proterozoic crust has been tectonically reactivated and has a thick sedimentary cover. Inside the Proterozoic domains, V_P/V_S tends to increase with increasing crustal thicknesses. The observed positive trend is robust and required by the data, we recall that our technique would tend to generate anticorrelated measurements. The average Poisson ratio of the Proterozoic 1 group is 0.26, while it is about 0.28 for the Proterozoic 2 group. These values are in good agreement with the global averages of 0.29 ± 0.02 for the Precambrian shields and 0.27 ± 0.03 for the Proterozoic platforms, given by Zandt and Ammon [6]. In contrast to the Precambrian domains, in the Phanerozoic provinces, which represent the eastern part of Australia, V_P/V_S tends to decrease with increasing crustal thicknesses. In this region, the crustal thickness does not exceed 40 km. From these measurements alone it is difficult to say if there is a bimodality or if there is a continuous trend. However, as will be discussed below, a negative trend is consistent with other evidence.

7. Discussion and concluding remarks

Since the mineralogical composition plays a key role in determining σ, the study of the variations of σ with the geology of the crust should provide important constraints regarding the formation of the continental crust and its evolution. Let us first

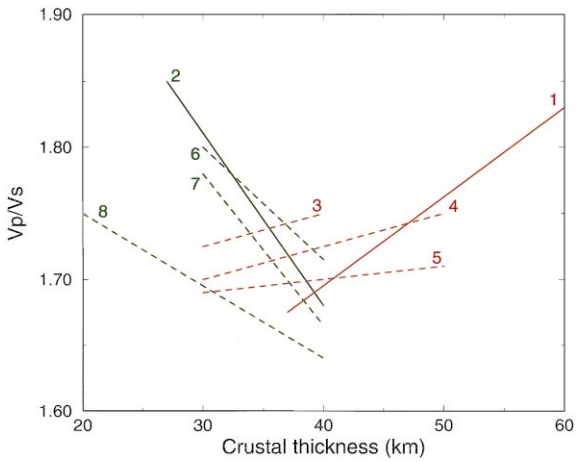

Fig. 8. Trends for different tectonic units. 1: North Australian craton. 2: Eastern Australia. 3–5: Siberian cratons. 6–8: Siberian Cenozoic basins (3–8 after Egorkin [26]).

consider the relative variations of σ as a function of crustal thickness inside a well defined geologic province. An increase of σ with increasing crustal thickness in the Proterozoic provinces is most easily explained by an increase of the thickness of a mafic lower crust, characterized by a granulite composition and a high σ. The large crustal thicknesses in the North Australian craton, which has remained stable since its formation, could result from the underplating of mafic and ultramafic rocks as proposed by Drummond and Collins [15]. Durrheim and Mooney [21] pointed out that the underplating of ultramafic rocks which characterizes the Proterozoic crust seems to be absent in the Archean crust. In their model of crustal evolution, the different thickness of the Archean and Proterozoic crusts, clearly expressed in Australia, results from the thermal history of the mantle. The extraction of the crust from eruptions of komatiitic lavas during the Archean produced an ultradepleted refractory lithosphere which prevented further production of basaltic melts. In contrast, the Proterozoic crust formed on top of a fertile mantle which can melt and produce basaltic underplating. A possible mechanism for producing a decrease of σ with a decrease of crustal thickness is crustal heating and differentiation as proposed by Meissner [23]. In this model, a thermal event heats the crust and produces melting. The light melt migrates to the upper crust and a refractory residue is left and is incorporated into the mantle. As a result, the Moho moves upward and the crust is thinner with a more felsic composition (and therefore a lower σ) than the original crust. In such a scenario, the seismic crust–mantle boundary could be different than the petrological crust–mantle boundary. From the analysis of high pressure xenoliths, Griffin and O'Reilly [24] argue that the spinel lherzolite to garnet lherzolite transition may be interpreted as the Moho in hot areas, while in cold areas, a mafic lower crust may be in the eclogite facies and would thus be defined seismically as mantle.

On the basis of the data from Australia alone, these relationships are tentative. Interestingly, however, a similar trend of increasing σ with increasing crustal thickness is observed in deep seismic soundings (DSS) of the Siberian platform (fig. 11 in Egorkin et al. [25] and fig. 4 in Egorkin [26]), which are, to our knowledge, the only other available studies that present comparable data (Fig. 8). For the DSS studies, the errors in V_P/V_S are about 0.5% and the errors in depth are less than 1% (Egorkin, personal communication) so this trend is robust and well documented. Since these studies were based on the analysis of different seismic phases (reflected and refracted P and S waves) with different data analysis techniques (2D travel time and waveform inversions), it is very unlikely that the trend observed in both studies is an artefact. This also suggests that the positive trend is perhaps a ubiquitous property of the Proterozoic crust. It would be very interesting to investigate other regions such as South Africa or North America, which are particularly favorable because of the large number of high quality broadband stations sampling different tectonic provinces of various age.

In contrast, the crust of the Paleozoic Siberian plate shows a decrease of σ with an increase of crustal thickness [25,26]. This tendency is also consistent with our dataset for Australia, but the scatter in our results and the limited number of stations prohibits further quantification. The observed scatter for the stations in Australia probably results from the sampling of very different tectonic provinces of Phanerozoic age. The decrease of V_P/V_S with increasing crustal thickness requires an increasing proportion of the felsic crustal component. Crustal thickening by stacking two upper crusts during orogeny is an efficient mechanism to generate a thick crust with low V_P/V_S. Subsequent erosion will progressively remove the felsic component and will make V_P/V_S increase while the crustal thickness will decrease to reach the isostatic equilibrium. Therefore, the pronounced anticorrelation between V_P/V_S and crustal thickness may be characteristic of a crust that experienced (recent) orogenic activity. The different trend observed for the Archean and Proterozoic crusts may simply reflect that cratonic crust tends to be stable and less prone to be involved in orogeny. If this is correct then the distinction between the two trends may not depend as much on crustal age as on the mechanical be-

havior of the crust and the underlying lithosphere. From surface wave inversions, Simons et al. [17] inferred a thick (250 km) high wave speed lithosphere beneath the Central Proterozoic region and a thin (less than 100 km) lithosphere under the Phanerozoic region, even though the difference in the elastic thickness of the lithosphere is less dramatic [27].

The existence of a correlation (or anticorrelation) between V_P/V_S and the crustal thickness strongly suggest that the SiO_2 content has a dominant effect on the average elastic properties of the crust, as shown by experimental studies on rocks with SiO_2 contents larger than 55% [4]. If this is true, then the abundance of SiO_2 has to be greater than 55% and it is possible to measure it directly from seismic data [26]. This conclusion is in good agreement with the average continental crust composition estimated by Rudnick and Fountain [2] in which the SiO_2 content is 59.1%.

Acknowledgements

This research was supported by the David and Lucile Packard Foundation and a Lavoisier Fellowship. The portable stations of the SKIPPY experiment, which was proposed and managed by RvdH, were funded by the Australian National University. We are indebted to Dr. Anatoly Egorkin for pointing us to his 1998 paper and for discussion of his results. The manuscript benefitted from the comments of two anonymous reviewers and from discussions with Francis Albarède and Roberta Rudnick at different stages of this work.*[FA]*

References

[1] R.L. Rudnick, Making continental crust, Nature 378 (1995) 571–577.
[2] R.L. Rudnick, D.M. Fountain, Nature and composition of the continental crust: a lower crustal perspective, Rev. Geophys. 33 (1995) 267–309.
[3] N.I. Christensen, W.D. Mooney, Seismic velocity structure and composition of the continental crust: a global view, J. Geophys. Res. 100 (1995) 9761–9788.
[4] N.I. Christensen, Poisson's ratio and crustal seismology, J. Geophys. Res. 101 (1996) 3139–3156.
[5] T.J. Clarke, P.G. Silver, Estimation of crustal Poisson's ratio from broad band teleseismic data, Geophys. Res. Lett. 20 (1993) 241–244.
[6] G. Zandt, C.J. Ammon, Continental crust composition constrained by measurements of crustal Poisson's ratio, Nature 374 (1995) 152–154.
[7] R. van der Hilst, B. Kennett, D. Christie, J. Grant, Project SKIPPY explores the mantle and lithosphere beneath Australia, in: EOS, Trans. Am. Geophys. Union 75 (1994) 180–181.
[8] T. Shibutani, M. Sambridge, B. Kennett, Genetic algorithm inversion for receiver functions with application to crust and uppermost mantle structure beneath eastern australia, Geophys. Res. Lett. 23 (1996) 1829–1832.
[9] G. Clitheroe, O. Gudmundsson, B.L.N. Kennett, The crustal structure of Australia, J. Geophys. Res. 105 (2000) 13,697–13,713.
[10] S. Chevrot, N. Girardin, On the identification of reflected and converted waves from receiver functions, Geophys. J. Int. 141 (2000) 801–808.
[11] A.P. Tarkov, V.V. Vavakin, Poisson's ratio behaviour in crystalline rocks: application to the study of the Earth's interior, Phys. Earth Planet. Inter. 29 (1982) 24–29.
[12] T. Watanabe, Effects of water and melt on seismic velocities and their application to characterization of seismic reflectors, Geophys. Res. Lett. 20 (1993) 2933–2936.
[13] T.J. Owens, G. Zandt, Implications of crustal property variations for models of Tibetan plateau evolution, Nature 387 (1997) 37–43.
[14] G. Zandt, S.C. Myers, T.C. Wallace, Crust and mantle structure across the Basin and Range-Colorado plateau boundary at 37°N latitude and implications for Cenozoic extensional mechanism, J. Geophys. Res. 100 (1995) 10,529–10,548.
[15] B.J. Drummond, C.D.N. Collins, Seismic evidence for underplating of the lower continental crust of Australia, Earth Planet. Sci. Lett. 79 (1986) 361–372.
[16] L. Zhu, H. Kanamori, Moho depth variation in southern California from teleseismic receiver functions, J. Geophys. Res. 105 (2000) 2969–2980.
[17] F.J. Simons, A. Zielhuis, R.D. van der Hilst, The deep structure of the Australian continent from surface wave tomography, Lithos 48 (1999) 17–43.
[18] G. Clitheroe, O. Gudmundsson, B.L.N. Kennett, Sedimentary and upper crustal structure of Australia from receiver functions, Austr. J. Earth Sci. 47 (2000) 209–216.
[19] C.D.N. Collins, The nature of the crust–mantle boundary under Australia from seismic evidence, in: B.J. Drummond (Ed.), The Australian Lithosphere, Geol. Soc. Aust. Spec. Publ., 1991, pp. 67–80.
[20] B. Efron, R. Tibshirani, Statistical data analysis in the computer age, Science 253 (1991) 390–395.
[21] R.J. Durrheim, W.D. Mooney, Archean and Proterozoic crustal evolution: evidence from crustal seismology, Geology 19 (1991) 606–609.

[22] J.S. Myers, Precambrian history of the west Australian craton and adjacent provinces, Annu. Rev. Earth Planet. Sci. 21 (1993) 453–485.
[23] R. Meissner, The Continental Crust, Academic Press, New York, 1986.
[24] W.L. Griffin, S.Y. O'Reilly, Is the continental Moho the crust–mantle boundary?, Geology 15 (1987) 241–244.
[25] A.V. Egorkin, S.K. Zuganov, N.I. Pavlenkova, N.M. Chernyshov, Results of lithospheric studies from long-range profiles in Siberia, Tectonophysics 140 (1987) 29–47.
[26] A.V. Egorkin, Velocity structure, composition and discrimination of crustal provinces in the former Soviet Union, Tectonophysics 298 (1998) 395–404.
[27] F.J. Simons, M.T. Zuber, J. Korenaga, Isostatic response of the Australian lithosphere: estimation of effective elastic thickness and anisotropy using multitaper spectral analysis, J. Geophys. Res. 105 (2000) 19,163–19,184.